

Electrooptic Polarization Modulation in Multielectrode $\text{Al}_x\text{Ga}_{1-x}\text{As}$ Rib Waveguides

F. K. REINHART, MEMBER, IEEE, RALPH A. LOGAN, SENIOR MEMBER, IEEE, AND W. ROBERT SINCLAIR

Abstract—A single mode rib waveguide (RWG) polarization modulator is described with a measured extinction ratio $\gtrsim 27$ dB, a power conversion ≈ 0.99 , and a switching voltage of 12.5 V at $\lambda = 1.064 \mu\text{m}$. The modulator is based on a modified step $\Delta\beta$ -reversal configuration. Contact with CdO and an Au overlay ensures low optical losses ($\lesssim 1 \text{ cm}^{-1}$) for both polarizations.

We report on a single mode rib waveguide (RWG) polarization modulator (POLAM) with a mode power modulation depth ≈ 0.99 , an extinction ratio $\gtrsim 27$ dB, a switching voltage $V_{\pi} \approx 12.5$ V at the test wavelength, $\lambda = 1.064 \mu\text{m}$, and a projected insertion loss < 1.5 dB. The POLAM consists of a RWG formed on $\text{Al}_y\text{Ga}_{1-y}\text{As}$ ($y = 0.15$) single heterostructure waveguide with $\text{Al}_x\text{Ga}_{1-x}\text{As}$ ($x = 0.2$) cladding grown on (110) oriented GaAs substrates. The electrodes are separated by about 1.2 mm, as discussed below, and consist of a highly conductive low optical loss CdO layer with an Au overlay. Capacitance values of ≈ 0.5 pF are estimated per RWG electrode for a two electrode section switch.

Previously demonstrated high performance $\text{Al}_x\text{Ga}_{1-x}\text{As}$ waveguide polarization (110) p-n junction modulators [1], [2] require nearly degenerate TE and TM modes. This was achieved with low differences between the Al concentrations x and y of the cladding and waveguide layers, respectively. The resulting planar guided modes are only weakly bound which makes it difficult to control the lateral guiding and the device capacitance because a relatively thick top cladding layer ($\gtrsim 2 \mu\text{m}$) has to be etched down to about 0.3 μm . A thick top cladding layer is needed to prevent high TM mode losses by the metallic contacts.

This novel device is fully integrable in a monolithic optical circuit [2] and not only permits the designer considerably more freedom than previous approaches, but also eliminates the above problems. The integrable POLAM is expected to become very important in single mode fiber optics systems to control or restore the polarization of the light [3], [4]. The potential high speed of the RWG-POLAM also may readily lend itself to high speed intensity and/or wavelength envelope modulation [2].

The structure, a schematic of which is shown by Fig. 1(a) and (b), was grown by liquid phase epitaxy (LPE), and 5 μm wide RWG were formed by the standard multiple anodization

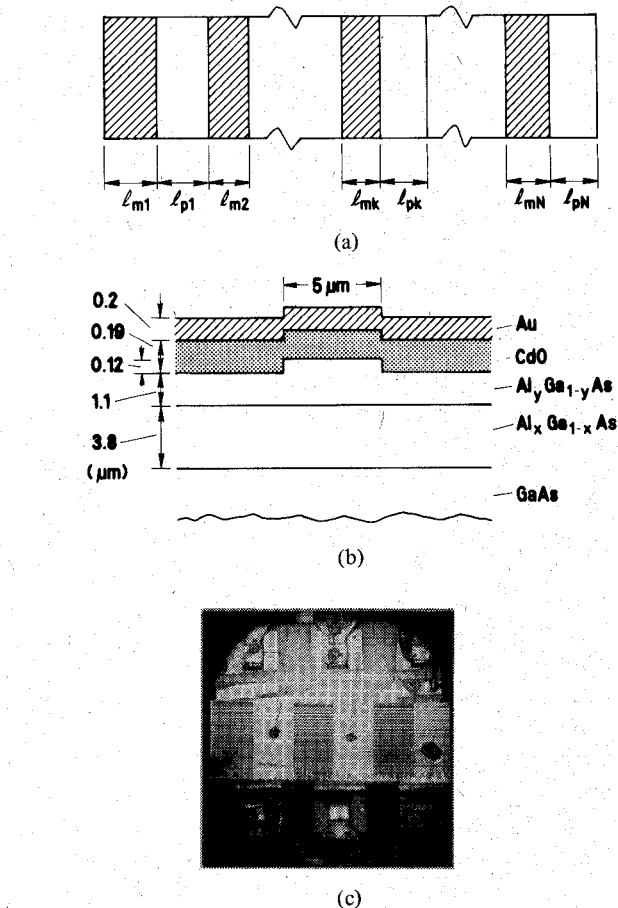


Fig. 1. Cross sections of the multielectrode rib waveguide modulator. (a) Schematic top view of the electrode arrangement. The shaded portions are the N sections of the CdO-Au overlay. Light propagation is from left to right. (b) Schematic cross section of a rib waveguide with CdO-Au contacts. (c) Photograph of an actual device with three modulator sections (bright areas with contact wires attached) mounted on a holder. The RWG's are visible as fine bright lines.

procedure [5]. The quality of LPE layers on (110) substrates generally is comparable to that of the conventional (100)-orientation. The RWG height (0.12 μm) was chosen to form low loss ($\lesssim 1 \text{ cm}^{-1}$) single mode RWG. The loss is expected to be dominated by the planar guide losses. CdO was sputtered to form a heterojunction barrier after carefully removing the photoresist and anodized oxide. CdO serves as a transparent electrode that hardly contributes to the optical loss of the TE and TM modes. A gold overlay of 0.2 μm facilitates the formation of electrical contacts. Electrode patterns again were

Manuscript received August 31, 1981; revised November 23, 1981. The authors are with Bell Laboratories, Murray Hill, NJ 07974.

formed by photolithographic masking and etching to define electrode lengths $l_m = 1.21$ mm and electrode spacings $l_p \approx 1.23$ mm. The devices were finally lapped and mounted on a modified "solar flare" integrated circuit holder [Fig. 1(c)] and tested electrically and optically in standard fashion.

Typical forward voltages at $10 \mu\text{A}$ current were 0.5 V. Reverse breakdown voltages on contact pads as large as 2 mm^2 were in excess of 15 V with n-type layers doped near 10^{16} cm^{-3} . The doping profile indicates a significant increase to 10^{17} cm^{-3} near the waveguide-cladding interface.

Accurate knowledge of the thickness and the Al composition of the waveguide and cladding is necessary to design the POLAM. In the analysis of the problem we also found that mechanical stresses due to differences of the thermal expansion coefficients of the layers must be taken into account [6]. The dominant contribution to the stress birefringence arises from the guide layer structure itself because $\text{Al}_x\text{Ga}_{1-x}\text{As}$ layers are lattice matched at growth temperature $\approx 850^\circ\text{C}$, but not at room temperature $\approx 22^\circ\text{C}$. Fluctuations of the room temperature by $\pm 4^\circ\text{C}$ affect the stress birefringence by less than 1 percent. With a waveguide layer thickness of $2w = 1.2 \mu\text{m}$ of $\text{Al}_{0.15}\text{Ga}_{0.85}\text{As}$, a cladding thickness of $3.8 \mu\text{m}$ of $\text{Al}_{0.2}\text{Ga}_{0.8}\text{As}$, and GaAs substrate thickness of $400 \mu\text{m}$, we calculate the modal phase difference between the TE and TM modes due to the stress birefringence for $E_J = 0$ as -2.4 rad/mm using Feldman *et al.*'s [7] photoelastic coefficients. The calculated modal phase difference including a CdO layer of $0.19 \mu\text{m}$ thickness and a thick Au layer $\gtrsim 0.2 \mu\text{m}$ is about 4 rad/mm . This results in a net modal phase difference $\beta_{\text{TE}} - \beta_{\text{TM}} = 1.6 \text{ rad/mm}$, where $\beta_{\text{TE,TM}}$ stand for the propagation constants of the TE and TM modes. Since this modal phase difference is quite sensitive to fluctuations in $2w$, x , and y , it is not unreasonable to expect sizable fluctuations of $\beta_{\text{TE}} - \beta_{\text{TM}}$. Measurements on a wafer indicated variations of nearly $\pm 1.8 \text{ rad/mm}$ yielding extremes of $-0.2 < \beta_{\text{TE}} - \beta_{\text{TM}} < 3.4 \text{ rad/mm}$. This range indicates that it is feasible to fabricate nearly phase matched POLAM, but also points to the desirability of having $(\beta_{\text{TE}} - \beta_{\text{TM}})$ adjustable to make up for uncontrolled differences.

The new device can be viewed as an analog to the modified $\Delta\beta$ -reversal switch [8], if one considers only a few electrodes. In the limiting case of very strong nondegeneracy, it is better regarded as a periodic coupler switch, where phase matching is achieved by the periodic arrangement of the grating [3]. As described in detail by [1], the polarization modulation is a direct result of the interference of the new eigenmodes created by the application of the junction electric field E_J along the (110)-direction. The principal axis of the optical dielectric tensor lie along the [110]-direction and in the (110) plane with angles of $\pm 45^\circ$ to E_J . As discussed above, the POLAM generally shows a significant splitting of the unperturbed ($E_J = 0$) TE and TM eigenmodes, and thus a simple electrode section can only achieve limited switching. Full switching could be restored by introducing sections where the sign of E_J is reversed alternately as is done in the step $\Delta\beta$ -reversal switches [9]. Unfortunately, this is not possible with planar electrode geometry of the POLAM, nor is it possible to use the simple modified step- $\Delta\beta$ reversal arrangement [8] because of the collinear propagation of the TE and the TM

modes. These problems are simply overcome by separating the electrode (or modulator) sections by a proper amount to permit a proper phase adjustment of the modes before entering the following modulator sections. In this way it is possible to maintain the sense of polarization rotation in the electrode section. Complete polarization switching will then be obtained with a sufficient number of sections that need not be identical.

The theory of a single mode (per polarization) N -electrode section device such as shown in Fig. 1(a) is straightforward using a conventional matrix approach. Input and output fields $E_{(\text{TE},\text{TM})}^{(\text{in},\text{out})}$ are related by the following matrix equation

$$\begin{bmatrix} E_{\text{TE}}^{\text{out}} \\ E_{\text{TM}}^{\text{out}} \end{bmatrix} = A \begin{bmatrix} E_{\text{TE}}^{\text{in}} \\ E_{\text{TM}}^{\text{in}} \end{bmatrix} \quad (1)$$

where A is the field transmission matrix of the device. As indicated by Fig. 1(a), the device can be subdivided into N individual sections of identical form which can be represented by a matrix $A_k (k = 1, 2, \dots, N)$. The matrix A is then obtained as a product of matrices

$$A = \prod_{k=1}^N A_k. \quad (2)$$

The matrix of the k th section is given by

$$A_k = \underbrace{\begin{bmatrix} \exp(-i\phi_{p,k}) & 0 \\ 0 & \exp(i\phi_{p,k}) \end{bmatrix}}_{\text{phasing section}} \cdot \underbrace{\begin{bmatrix} a_k & b_k \\ b_k & a_k^* \end{bmatrix}}_{\text{electrode section}} \exp(-i\theta_k) \quad (3)$$

where

$$2\phi_{p,k} = [\beta_{p\text{TE},k} - \beta_{p\text{TM},k}] l_{p,k}, \quad (4)$$

$$2\phi_{m,k} = [\beta_{m\text{TE},k} - \beta_{m\text{TM},k}] l_{m,k}, \text{ at } E_J = 0, \quad (5)$$

and

$$\theta_k = \frac{1}{2} [[\beta_{m\text{TE},k} + \beta_{m\text{TM},k}] l_{m,k} + [\beta_{p\text{TE},k} + \beta_{p\text{TM},k}] l_{p,k}] \quad (6)$$

with $\beta_{m,\text{TE,TM},k}$, k standing for the propagation constants for the TE and TM modes of the respective k th phasing (p) and modulator (m) sections.

$$a_k = \cos \psi_k - i \frac{r_k}{\sqrt{1+r_k^2}} \sin \psi_k \quad (7)$$

$$b_k = -i \frac{\sin \psi_k}{\sqrt{1+r_k^2}} \quad (8)$$

where

$$\psi_k^2 = \phi_{m,k}^2 + (\kappa_k l_{m,k})^2 \quad (9)$$

and

$$r_k = \phi_{m,k} / \kappa_k l_{m,k} \quad (10)$$

where $\kappa_k l_{m,k}$ is the electrooptically induced phase difference in the degenerate case [1]. With the average junction electric field in the k th section $\bar{E}_{J,k}$ parallel to the crystallographic [110]-direction, we can write

$$2\kappa_k = \Gamma(2\pi/\lambda)n^3 r_{41} \bar{E}_{J,k} \quad (11)$$

where $r_{41} \approx -1.4 \times 10^{-10}$ cm/V the electrooptic coefficient; $n \approx 3.402$ the index of refraction of the waveguide layer, and Γ is the overlap of the junction electric field with the optical field. Since we are only interested here in TE and TM modes, we may disregard the common phase factor and represent the ideal through (||) state by $A_{||} = \begin{bmatrix} 1 & 0 \\ 0 & 1 \end{bmatrix}$, and the ideal crossed state (X) by $A_X = \begin{bmatrix} 0 & i \\ i & 0 \end{bmatrix}$.

In the case of identical sections, the section index k is no longer needed, and it is easy to establish guidelines to achieve perfect switching which is always obtained by switching from $\bar{E}_J \approx 0$ to $\bar{E}_J \lesssim \bar{E}_{J,\max}$. $\bar{E}_{J,\max}$ is given by either the maximum field permitted in terms of a maximum acceptable switching energy or the maximum field that the semiconductor may sustain without breakdown due to avalanche carrier multiplication or tunneling. By inspection of (1) it is readily observed that ideal switching is always possible with $2\phi_p = \pi$ and $r^* = \cot \pi/2N = \phi_{m,\max}/k_{\max} l_m$, as given in Table I for up to five identical sections. Also shown in Table I is the ratio $(l_m/l_p)_{\min} = r^*/\sqrt{1+r^{*2}}$ and $2\phi_{m,\max}$ for an assumed $2\kappa_{\max} l_m = \pi$ that is easily reached with $\bar{E}_J = 15$ V/ μm and a length $l_m \approx 1$ mm. With these values we should readily achieve high performance devices.

From this analysis we also recognize that this device can also be efficiently used as a general polarization transformer [4] if we can also modulate $\phi_{p,k}$. Possibilities exist for this case but they cannot be discussed here. It is, however, important to take note that static tuning of $\phi_{p,k}$ will be useful to make up for design tolerances. Tuning also allows one to compensate for fabrication tolerances as discussed above.

Optical tests of the devices were performed at $\lambda = 1.064 \mu\text{m}$ in a standard manner using an external Glan-Thompson analyzer prism. The results for a two section device with $l_m = 1.21$ mm and $l_p = 1.23$ mm are shown in Fig. 2, with identical electrode voltages. Both the || and X states indicate an energy exchange ratio $F \geq 0.98$ and $V_\pi \approx -12.5$ V. With dissimilar electrode voltages -11.3 and -12.4 V, respectively, we get $F \approx 0.99$, which resulted in a substantially better extinction ratio (20 dB instead of 17 dB) when switching from the || to the X state. Switching from the X to the || state resulted in an extinction ratio in excess of 27 dB. These results demonstrate that even imperfect design of the POLAM can yield excellent performance similar to the near degenerate case. These results are consistent with a uniform phase difference $\beta_{TE} - \beta_{TM} \approx 2$ rad/mm ($E_J = 0$) over the phase and modulator sections. A slight adjustment to $\beta_{TE} - \beta_{TM} \approx 2.041$ rad/mm ought to result in perfect modulation for the given l_m/l_p ratio.

Tests on individual modulator sections resulted in sizable polarization modulation and no measurable additional loss due to the electrodes. Energy exchange ratios varied from RWG to RWG indicating sizable variations of the phase mismatch. In

TABLE I

N	r^*	$(l_m/l_p)_{\min}$	$2\phi_{m,\max}$
1	0	indefinite	0
2	1	0.7071	π
3	$\sqrt{3}$	0.8660	5.4414
4	$\frac{1+\sqrt{2}}{2}$	0.9239	7.5845
5	$\frac{\sqrt{5}+\sqrt{20}}{5}$	0.9511	9.6688

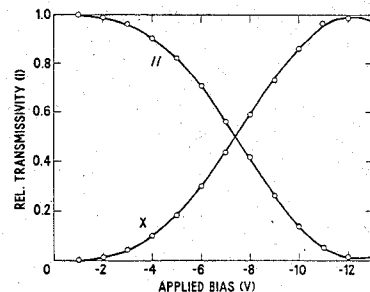


Fig. 2. Relative transmissivity as a function of applied bias of a two section modulator. The two curves represent the || and X analyzer cases.

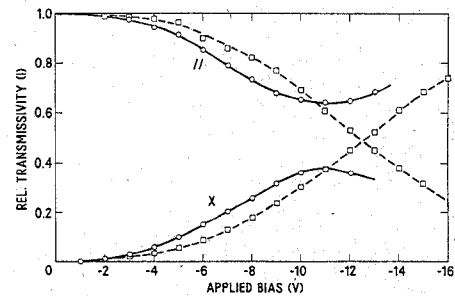


Fig. 3. Relative transmissivity as a function of applied bias for an incorrectly designed phase section. One electrode modulator data (dashed line) and two electrode modulator data (solid curve) for both || and X states. The two electrode case uses a second electrode added to the single electrode case.

Fig. 3 the results of the || and X are shown for an improperly phased case. The dashed line represents the smooth fit through the one electrode data given by the squares. The two electrode data (circles) were taken with identical voltages, where one of the electrodes is identical to the one that produced the square data points. The two electrode combination is worse than the one electrode case because $F \approx 0.37$ at the extrema at $V_\pi = -11$ V for two modulating sections. From these data we estimate the phase mismatch for this waveguide as 0.68 rad/mm under the assumption of uniform phase mismatch in the phasing and modulator sections. This result demonstrates the importance of the phasing section which is clearly incorrect in this RWG.

Additional tests with tuning ϕ_p or λ could serve to prove that $F > 0.99$ could be achieved. Using four multimode sections we would expect to reduce V_π to about 5 V. Reduction of the CdO overlap over the RWG section has been independently demonstrated and will serve to reduce the capacitance per electrode below 0.5 pF for 3 μm wide RWG [8]. This value is sufficiently low to permit effective high speed modula-

tion. According to our electrical data the overlap of the optical field with E_J is not optimal [10]. This suggests that the performance could be further increased by designing a switching device such as to switch from a high bias point to an even higher bias value. We estimate an improvement of the necessary switching voltage difference by up to a factor of two. Modulation of the phasing section would facilitate the design of such a modified device [11] and also make it insensitive to fabrication tolerances.

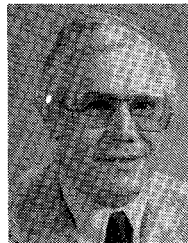
In conclusion, we have successfully demonstrated a new RWG polarization modulator approach that permits easy application in monolithic optical circuits. The switching energies are expected to be in the order of 10 pJ at $\lambda \cong 1.06 \mu\text{m}$. We also expect that this type of switch is readily adaptable to different semiconductor compounds notably to the InGaAsP-InP compound system.

ACKNOWLEDGMENT

The authors would like to express their sincere thanks to H. G. White for his crystal growth efforts and J. J. Schott for his expert technical assistance in handling and assembling the devices.

REFERENCES

- [1] J. C. McKenna and F. K. Reinhart, "Double-heterostructure GaAs-Al_xGa_{1-x}As [110] p-n junction-diode modulator," *J. Appl. Phys.*, vol. 47, pp. 2069-2078, 1976.
- [2] F. K. Reinhart, "Prospects of monolithic optical integration," *Proc. SPIE*, vol. 272, pp. 66-75, 1981.
- [3] R. C. Alferness and L. L. Buhl, "Electrooptic waveguide TE \rightarrow TM mode converter with low drive voltage," *Opt. Lett.*, vol. 11, pp. 473-475, 1980.
- [4] R. C. Alferness, "Electrooptic guided-wave device for general polarization transformation," *IEEE J. Quantum Electron.*, vol. QE-17, pp. 965-969, 1981.
- [5] J. C. Shelton, F. K. Reinhart, and R. A. Logan, "Characteristics of rib waveguides in AlGaAs," *J. Appl. Phys.*, vol. 50, pp. 6675-6687, 1979.
- [6] F. K. Reinhart and R. A. Logan, "Interface stress of Al_xGa_{1-x}As-GaAs laser structures," *J. Appl. Phys.*, vol. 44, pp. 3171-3175, 1973.
- [7] A. Feldman and D. Horowitz, "Dispersion of the piezobirefringence of GaAs," *J. Appl. Phys.*, vol. 39, pp. 5597-5599, 1968.
- [8] J. C. Shelton, F. K. Reinhart, and R. A. Logan, "Rib waveguide switches with MOS electrooptic control for monolithic integrated optics in GaAs-Al_xGa_{1-x}As," *Appl. Opt.*, vol. 17, pp. 2548-2555, 1978.
- [9] H. Kogelnik and R. V. Schmidt, "Switched directional couplers with alternating $\Delta\beta$," *IEEE J. Quantum Electron.*, vol. QE-12, pp. 396-401, 1976.
- [10] L. O. Wilson and F. K. Reinhart, "Phase modulation nonlinearity of double-heterostructure p-n junction diode light modulators," *J. Appl. Phys.*, vol. 45, pp. 2219-2228, 1974.
- [11] F. K. Reinhart, unpublished.



F. K. Reinhart (S'62-M'63) was born in Bassersdorf, Switzerland in 1933. He received the dipl. Ing. degree in electrical engineering in 1958 and the Dr.sc.techn. degree in 1962 from the Swiss Federal Institute of Technology, Zurich, Switzerland.

In 1963 he joined Bell Laboratories, Murray Hill, NJ, where his work in the Solid State Electronics Research Laboratory centers on semiconductor device feasibility studies mostly for optical communications. In 1976 he was a Visiting Professor at the Institute of Applied Physics at the University of Berne, Berne, Switzerland.



Ralph A. Logan (M'73-SM'73) was born in Cornwall, Ont., Canada, on September 22, 1926. He received the B.Sc. and M.Sc. degrees in applied mathematics from McGill University, Montreal, P.Q., Canada, in 1947 and 1948, respectively; and the Ph.D. degree in physics from Columbia University, New York, NY, in 1952.

In 1952 he joined Bell Laboratories, Murray Hill, NJ. His work in the Solid State Electronics Research Laboratory at Bell includes studies of dislocations, p-n junctions, electroluminescence, and crystal growth to form optical communication devices.

Dr. Logan is a Fellow of the American Physical Society.



W. Robert Sinclair was born in Chicago, IL in 1924. He received the B.S. and Ph.D. degrees in chemistry from the University of Chicago, Chicago, IL, in 1945 and 1952, respectively.

In 1952 he joined Bell Laboratories, Murray Hill, NJ, where his work in the Electronic Materials Applications Research Department includes the preparation and characterization of semiconducting and superconducting thin films.

Dr. Sinclair is a member of the Electrochemical Society and the American Physical Society.